Clinical Cancer Research

Farnesyltransferase Inhibitors and Human Malignant Pleural Mesothelioma: A First-Step Comparative Translational Study

Alfredo Cesario, Alessia Catassi, Luigi Festi, et al.

Updated Version	Access the most recent version of this article at: doi:10.1158/1078-0432.CCR-04-1450

Cited Articles	This article cites 49 articles, 27 of which you can access for free at: http://clincancerres.aacrjournals.org/content/11/5/2026.full.html#ref-list-1
Citing Articles	This article has been cited by 1 HighWire-hosted articles. Access the articles at: http://clincancerres.aacrjournals.org/content/11/5/2026.full.html#related-urls

E-mail alerts	Sign up to receive free email-alerts related to this article or journal.
Reprints and Subscriptions	To order reprints of this article or to subscribe to the journal, contact the AACR Publications Department at pubs@aacr.org.
Permissions	To request permission to re-use all or part of this article, contact the AACR Publications Department at permissions@aacr.org.

Farnesyltransferase Inhibitors and Human Malignant Pleural Mesothelioma: A First-Step Comparative Translational Study

Alfredo Cesario,[1,5] **Alessia Catassi,**[2] **Luigi Festi,**[4]
Andrea Imperatori,[4] **Andrea Pericelli,**[4]
Domenico Galetta,[1] **Stefano Margaritora,**[1]
Venanzio Porziella,[1] **Vittorio Cardaci,**[5]
Pierluigi Granone,[1] **Lorenzo Dominioni,**[4] **and**
Patrizia Russo[3]

[1]Department of Surgical Science, Division of General Thoracic Surgery, Catholic University, Rome, Italy; [2]Department of Biology, University of Genoa; [3]Laboratory of Translational Research B (Lung Cancer), Department of Integrated Medical Oncology, National Cancer Institute, Genoa, Italy; [4]Center of Thoracic Surgery, University of Insubria, Varese, Italy; and [5]Pulmonary Rehabilitation, IRCCS San Raffaele, Rome, Italy

ABSTRACT

It is known that the potential clinical use of farnesyltransferase inhibitors (FTI) could be expanded to include cancers harboring activated receptor tyrosine kinases. Approximately 70% of malignant pleural mesotheliomas (MPM) overexpress epidermal growth factor receptors (EGFR) and a subset express both EGFR and transforming growth factor α (TGF-α), suggesting an autocrine role for EGFR in MPM. We checked on MPM cells (10 human cell lines, 11 primary cultures obtained by human biopsies, and 7 short-term normal mesothelial cell cultures) concerning the following: (*a*) the relative overexpression of EGFR (Western blotting, flow cytometry, immunohistochemistry), (*b*) the relative expression of EGFR ligands (EGF, amphiregulin, TGF-α, ELISA), (*c*) the relative increase of the activated form of Ras (Ras-bound GTP) after EGF stimulation (Ras activation assay), (*d*) the efficacy of five different FTIs (HDJ2 prenylation, cell cytotoxicity, and apoptosis using ApopTag and gel ladder). EGFR was overexpressed in MPM cells compared with normal pleural mesothelial cells in equivalent levels as in non–small cell lung cancer cells A549. MPM cells constitutively expressed EGFR ligands; however, Ras activation was attenuated at high EGF concentrations (100 ng/mL). Growth of MPM cells was substantially not affected by treatment with different FTIs (SCH66336, BMS-214662, R115777, RPR-115135, and Manumycin). Among these, BMS-214662 was the only one moderately active.

BMS-214662 triggered apoptosis in a small fraction of cells (not higher than 30%) that was paralleled by a slight decrease in the levels of TGF-α secreted by treated MPM cells. Our data highlighted the concept that the same signaling pathway can be regulated in different ways and these regulations can differ between different cells of different origin.

INTRODUCTION

The incidence of malignant pleural mesothelioma (MPM), a primary tumor of the pleural, peritoneal, and pericardial cavities, with an estimated incidence of 2,000 to 3,000 cases annually in the United States, is relatively high in Italy: about 1,000 patients are observed every year. The total number of male deaths from pleural mesothelioma in France, Germany, and Italy has continued to increase during the last decade of the 20th century, growing from ∼ 7,550 in 1985-1989 to 8,750 in 1990-1994, and 9,550 in 1995-1999 (1). However, for the latest period, all the observed values were lower than predicted (2). This, together with the stabilization of age-standardized mortality rates and the consistent decrease in mortality at younger ages, supports the hypothesis that the rising trend in deaths from mesothelioma in men could level off in the near future (3).

A unique feature of MPM is its strong relationship with asbestos fiber exposure, which has recently led to great public concern in view of the ubiquitous presence of that mineral. Exposure can be occupational, environmental, or even familial by household contamination. The median interval between onset of symptoms and death is usually 6 to 8 months (4) and long-term survivors are rare. MPM usually progresses locally, causing death by cardiac/respiratory failure in most cases.

To date there is no standard effective treatment for MPM (5, 6). Complex therapeutic protocols, including the combination of surgery, chemotherapy, and radiation therapy, as pioneered by Sugarbaker et al. (7) in 1991 in highly selected groups of patients represent the best-documented potentially curative approach, with 5-year survival not exceeding 15%. Such dismal prognosis status despite the aggressive therapeutic effort represents the *rationale* to foster investigation (6).

Very recently, some interesting positive results have been obtained by introducing new chemotherapeutic agents such as pemetrexed + cisplatin supplemented with folate and B12 (8), but the profound sense of nihilism surrounding treatment of this disease remains and the state of the art still seems unsatisfactory.

Moreover, knowledge of the biology of this cancer is still somewhat confused. Further efforts in the evaluation of the basics and of the response of this tumor to the newly proposed therapies are needed.

Specialized information is necessary for the planning of studies with a translational attitude, based both on clinical failure experiences and on advances in basic molecular oncology.

To date, we know that ∼ 70% of MPMs have high levels of expression of the epidermal growth factor receptor (EGFR), and

a subset of cell lines derived from MPM patients express both EGFR and transforming growth factor α (TGF-α) suggesting an autocrine role for EGFR in MPM (9–11).

Ras-mitogen-activated protein kinase pathway is an important signaling pathway activated by EGF as shown in Fig. 1 (12–17). Studies have shown that farnesylation of Ras is the obligatory first step in a series of posttranslational modifications leading to membrane association which, in turn, determines the switch from an inactive to an active Ras-GTP bound form (18–22). Based on the theoretical assumption that preventing Ras farnesylation might result in the inhibition of Ras functions, a range of farnesyl-transferase inhibitors (FTI) have been synthesized (21, 22).

Farnesylated proteins such as Ras, RhoB, the centromere-binding proteins CENP-E and CENP-F, the phosphatases PRL1, 2 and 3, the chaperone protein DnaJ, and Rheb are involved in cell growth crucial pathways and may represent an ideal target for

Fig. 1 EGFR and Ras cascade. The adaptor protein growth factor receptor binding protein 2 (*Grb2*) plays a critical role in coupling signal from EGFR kinase with Ras. Grb2 contains a single SH2 domain flanked by two Src homology 3 (*SH3*) domains. The SH2 domain of Grb2 recognizes and binds to specific phosphotyrosine-containing motifs on EGFR, whereas the SH3 domains bind to the guanine nucleotide-releasing factor son of sevenless (*SOS*), which catalyzes the exchange of GDP to GTP on Ras, resulting in Ras activation (12–16). Interestingly, it has been reported that Grb2 directly binds to the cytoplasmic domain of EGFR at phosphorylated residues Tyr[1068] and Tyr[1086] to initiate the activation of the Ras-mitogen-activated protein kinase pathway. Ras, in turn, activates the downstream kinases sequentially, which eventually leads to the activation of mitogen-activated protein kinases/ERKs. ERKs phosphorylate transcription factors that regulate gene transcription (12–16).

novel molecular targeted therapies with a wide anticancer spectrum (21, 22). Preclinical experiments have confirmed that FTIs are able to effectively inhibit farnesylation of several targets, leading to powerful anticancer effect in a variety of cell lines and xenograft animal models (21, 22). Moreover, it is well known that FTIs block the growth of a variety of tumor cells without Ras activation (21, 22). It is possible that this occurs because activated receptor tyrosine kinases constitutively activate Ras that is then inhibited by FTIs; alternatively, FTIs may inhibit TGF-α and amphiregulin expression, as shown by Sizemore et al. (23). In support of this hypothesis, Noorgaard et al. (24, 25) reported that the FTI L744,382 decreases levels of TGF-α in mammary cystic fluid and inhibits the growth of mammary tumors in MMTV-TGF-α transgenic mice. Furthermore, we have shown that the FTI RPR-115135 inhibits the growth of MCF10A cells transfected with *erb-B2* gene (26).

In a translational attitude, Trombino et al. (27) and others (28–30) have focused attention on MPM. We studied 10 human MPM cell lines, 11 MPM cell lines in primary cultures obtained by human biopsies, and 7 short-term normal mesothelial cell cultures to investigate the following:

1. The relative overexpression of EGFR using different methodologies: Western blotting, flow cytometry, and immunohistochemistry;
2. The relative expression of EGFR ligands (TGF-α and amphiregulin) using ELISA;
3. The relative increase of the activated form of Ras (Ras-bound GTP) after EGF stimulation (Ras activation assay);
4. The relative extracellular signal-regulated kinase (ERK) activation after EGF stimulation (Western blotting);
5. The efficacy of five different FTIs using cell cytotoxicity assays, HDJ2 mobility shift, and apoptosis detection (ApopTag, gel ladder). The efficacy of other potential Ras-targeting agents such as methotrexate, which interferes with carboxymethyl transferase [3-(4,5-dimethylthiazol-2-yl)-5-(3-carboxymethoxyphenyl)-2- (4-sulfophenyl)-2*H*- tetrazolium, inner salt (MTS) assay and cloning in agar].

The results of this analysis are described herein.

MATERIALS AND METHODS

Cell Lines and Primary Cell Cultures. Human mesothelioma cancer cell line MSTO-211H, non–small cell lung cancer (NSCLC) A549 cell line, and human colon cancer HCT116 cell line were obtained from American Type Culture Collection (Rockville, MD). Human mesothelioma cancer cell lines H28, H513, H2052, and H290 were courtesy of Dr J.D. Minna (Hamon Center for Therapeutic Oncology Research, University of Texas Southwestern Medical Center, Dallas, Texas). Human mesothelioma cancer cell lines IST-MES-1, MPP-89, ZL55, and ZL34 were courtesy of Dr. S. Ferrini (National Institute for Research on Cancer, Genoa, Italy). They were grown in RPMI 1640 (Life Technologies, Inc., Grand Island, NY) supplemented with 10% non–heat inactivated fetal bovine serum (FBS, Life Technologies). Cell counts were determined using a Coulter Counter with Channelyzer attachment to monitor cell size (Coulter Electronics, Hialeah, FL). Cell membrane integrity was determined by trypan blue dye exclusion assay.

Tumor tissue samples from mesothelioma patients were taken from the operating room at room temperature immediately after resection. Primary cells were obtained as described previously (27). Briefly, the specimens were dissected with scalpels into <5-mm cubes. The pieces of tumor were placed in triple enzyme medium (1× collagenase, 1× hyaluronidase, and 1× DNase; Sigma, St. Louis, MO) in HBSS (Life Technologies) with a magnetic bar and were then spun on a stir plate at room temperature for 2 to 3 hours until most of the solid tumor was dissociated. The cells were filtered through a 70-μm nylon cell strainer (Becton Dickinson, Lincoln Park, NJ) and suspended in RPMI 1640 with 10% FBS (Life Technologies).

Normal pleural tissues samples were obtained from resected specimens of patients who underwent surgery for nonneoplastic reasons. Short-term mesothelial cell cultures were established as described previously (27) after triple enzyme medium (Sigma) disaggregation. Mesothelial cells were grown as primary cultures on fibronectin-coated culture flasks in RPMI 1640 supplemented with 20% heat-inactivated FBS (Life Technologies), epidermal growth factor (20 ng/mL), hydrocortisone (1 μmol/L) and insulin (10 μg/mL), transferrin (5 μg/mL), and gentamicin (50 μg/mL, Life Technologies) at 37°C in a humidified 5% CO_2 atmosphere. Fresh complete medium was replaced every 2 to 3 days until cells were confluent. Upon confluence the cells were lifted by 1× trypsin-EDTA (Life Technologies) and subcultured at 1:2 dilution. The cells were identified as mesothelial cells by immunocytochemical staining with antikeratin antibodies (Dako, Glostrup, Denmark). Third- to fourth-passage confluent cultures were used for binding assay and cell growth.

EGFR determination was evaluated by immunostaining, Western blot, and flow cytometry. Immunostaining against EGFR was done as follows: fixed cells were rinsed in cold PBS containing 0.5 mol/L glycine, blocked with PBS containing 1% bovine serum albumin and 5% FBS. The incubation was carried out overnight at 4°C in the primary antibody EGFR (SC-03; Santa Cruz Biotechnology, Santa Cruz, CA) diluted 1:200 in PBS-0.1% bovine serum albumin-1% FBS. After incubation, samples were rinsed with PBS and stained with the appropriate secondary anti-IgG, diluted 1:100 (Santa Cruz Biotechnology) in PBS containing 0.1% bovine serum albumin and 1% FBS. Specificity controls were done by use of normal serum as primary antibody or by omitting the incubation in the primary antibody. Peroxidase controls were done by preincubating cells in PBS containing 0.1% hydrogen peroxide before the incubation in the secondary antibody.

For Western blot analysis, equal amounts of protein were subjected to 12.5% SDS-PAGE and then transferred electrophoretically to a nitrocellulose membrane. Nonspecific binding sites were blocked with blocking buffer containing TBS and 0.1% Tween 20 with 5% nonfat milk powder for 2 hours at room temperature, and the blot was incubated with specific antibody in blocking buffer. The EGFR (SC-03) or the β-actin antibody (AC-15 (Sigma) was incubated at 4°C overnight. After washing, the blot was incubated with an appropriate secondary antibody (Santa Cruz Biotechnology) for 1 hour at room temperature. After extensive washing, detection was done using the enhanced chemiluminescence system with exposure to Hyperfilm MP.

For flow cytometry, cells were incubated in 1% bovine serum albumin in PBS for 30 minutes and then stained with the FITC-conjugated anti-EGFR monoclonal antibody (PharMingen, San Diego, CA; 1:50) for 1 hour on ice. As a negative control, an aliquot of the cells was stained with the FITC-conjugated monoclonal antibody of the same phenotype (PharMingen; 1:50). Flow cytometry was done on a FACScan analyzer (Becton Dickinson, Mountain View, CA), and median EGFR-positive values in cells were calculated by using the CellQuest program (Becton Dickinson).

Analysis of Growth Factor Release. MPM cell lines and primary MPM cells were seeded into 24-well culture trays, whereas primary pleural mesothelial cells were seeded into 24-well fibronectin-coated culture trays at 0.75×10^5 cells per well in complete medium, as described above, and cultured for 96 hours. After 24 hours, plating cells were treated for an additional 48 hours with FTI. The conditioned medium was then removed from the cells, clarified by centrifugation, and stored frozen until assay. ELISA kits for TGF-α (CN Biosciences, Nottingham, United Kingdom.), amphiregulin (R&D Systems, Abingdon, United Kingdom), and EGF were used according to the manufacturer's instructions; the minimum detectable amount of each factor in these assays was 10, 15, and 30 pg/mL, respectively.

Ras Activation Assay. A Ras activation assay kit was obtained from Upstate Biotechnology Inc. (Waltham, MA), and the experiment was conducted according to the manufacturer's protocol. Briefly, cells were serum starved overnight followed by growth factor stimulation (EGF for 10 minutes). Cells were lysed followed by addition of Raf-1 Ras-binding domain agarose to cell lysates followed by incubation for 30 minutes at 4°C. Beads were washed twice and the bound Ras was detected by incubation in SDS sample buffer and boiling followed by electrophoresis and Western blotting with an anti-Ras antibody (clone RAS 10).

Cell Proliferation Assay. All of the experiments for each drug were done at least twice with a minimum of six replicates per data point per experiment. Mesothelioma cell lines were plated with an eight-channel pipette at 250 cells per well in 96-well plates, whereas human normal mesothelial cells at 500 cells per well on fibronectin-coated 96-well plates. Drugs were added immediately after cell plating. The final medium volume of each well was 200 μL. At 10 days of incubation, an MTS-based assay, as described previously (27) was used to measure cell growth. Twenty microliters of MTS reagent (cell Titer 96 Aqueous; Promega Corporation, Madison, WI) were added per well, and absorbance at 490 nm was recorded 2 hours later.

Cell Proliferation in Soft Agar Assay. Primary human mesothelioma cells (106) were cultured in 60-mm dishes in 0.5% low-gelling agarose (Sea Plaque) on a base layer of 1% noble agar (Difco-BD, Franklin Lakes, NJ) in the presence of indicated amounts of FTI (added on day 1) or vehicle control in complete medium (according to American Type Culture Collection recommendations) and colonies were scored after 10 days. During the experiment, 0.5 mL of fresh complete medium (with or without drug) was added every 5 days. The cell clonogenic fraction was calculated using the following equation:

Clonogenic fraction

$$= (\text{Colonies counted}/\text{Number of cells seeded}) \times 100$$

Detection of Apoptosis. Apoptosis was detected with two different methods: ApopTag and internucleosomal DNA fragmentation.

ApopTag. After cytospinning the cells to slides, the ApopTag Peroxidase *in situ* apoptosis assay was done as described by the manufacturer (Intergen, Purchase, NY) and by ourselves previously (31). Briefly, 1.0×10^4 cells were cytospinned to the poly-L-lysine–precoated slides at $750 \times g$ for 5 minutes. The cells were fixed in 4% paraformaldehyde for 30 minutes. Cells were incubated in a humidified chamber with terminal deoxynucleotidyltransferase enzyme for 1 hour at 37°C (for the negative control, water was used instead of the enzyme), then soaked in a stop-wash buffer (Intergen) for 30 minutes, rinsed thrice in PBS, and finally incubated with antidigoxigenin-peroxidase (Intergen) at room temperature in a humidified chamber for 30 minutes. The brown color development was achieved by incubating for 6 minutes at room temperature with a substrate solution containing 0.008% 3,30-diaminobenzidine-tetrahydrochloride and 0.02% hydrogen peroxide. The slides were counterstained in a methyl green solution for 10 minutes and visualized and scored under a light microscope. One thousand cells were randomly scored per slide to evaluate dark brown color in the nuclei. Pictures were taken at 400× magnification.

Internucleosomal DNA Fragmentation. Internucleosomal DNA fragmentation was shown by the harvesting of total cellular DNA, as previously described (27). Briefly, adherent and detached cells were harvested separately, washed, and lysed with 50 mmol/L Tris (pH 7.5) 10 mmol/L EDTA, 0.5% Triton X-100, and 0.5 mg/mL proteinase K for 2 hours at 50°C. Samples were then extracted twice with phenol/chloroform/isoamyl alcohol and precipitated with ethanol. The pellet was resuspended in Tris-EDTA and 10 μg/mL Rnase A, and the DNA was separated on a 2% agarose gel.

Analysis of Protein Prenylation. Cells were treated with inhibitors for 24 hours and then lysed in radioimmunoprecipitation assay buffer [40 mmol/L Tris-HCl (pH 7.5), 150 mmol/L NaCl, 0.1% SDS, 0.5% sodium deoxycholate, 1% Triton X-100, and 0.1 mmol/L EDTA] and protease inhibitors. Lysates were subjected to SDS-PAGE using 8% precast Novex Tris-glycine gels (Invitrogen, Carlsbad, CA) and then immunoblotted using antibodies specific for HDJ2 (Lab Vision Inc., Fremont, CA). Blots were developed using alkaline phosphatase–conjugated anti-IgG (Cappel Laboratories, West Chester, PA) followed by detection with fluorescent alkaline phosphatase substrate (ECF, Amersham Pharmacia Biotech, Piscataway, NJ). Unfarnesylated and farnesylated proteins were distinguished by virtue of their different electrophoretic mobilities; thus the unfarnesylated forms of these proteins display reduced mobility in SDS-PAGE relative to their farnesylated versions.

p-ERK Detection. Standard protocols were used for Western blotting, as described above. A detergent-compatible protein assay kit (Bio-Rad, Hercules, CA) was used for quantitation of proteins. Western blots were developed with enhanced chemiluminescence reagents (Amersham). Anti p-ERK and anti total ERK antibodies were used (Santa Cruz Biotechnology).

Statistical Analysis. Student's *t* test ($P > 0.05$, not significant) was used.

RESULTS

EGFR Expression. The relative expression of EGFR in MPM cells (cell lines and primary cultures) as well as in primary short-term normal pleural mesothelial cells was determined using different methodologies: Western blotting, flow cytometry, and immunohistochemistry (Fig. 2).

A quantitative analysis of the intensity of the bands obtained by Western blotting (Fig. 2) revealed that the apparent EGFR/actin ratio was substantially near to 1.0 in human normal pleural mesothelial cells. In MPM cells, on the contrary, it was much higher than 1.0, such as in the NSCLC cell line A459 (positive control). These data suggest that in MPM EGFR is overexpressed in comparison with normal mesothelial cells at a level comparable with that of NSCLC cells, in agreement with data previously reported by Janne et al. (11).

Flow cytometry and immunohistochemistry confirmed Western blotting results (Fig. 2).

TGF-α, Amphiregulin, and EGF Release from Primary Pleural Mesothelial Cells, MPM Cell Lines, and Primary Cultures. Overexpression of released EGF or EGFR ligands (TGF-α and amphiregulin) was observed in MPM cells. In normal pleural mesothelial cells, their levels were at the limit of sensitivity of the assay (Table 1).

FTIs Sensitivity. Different FTIs [i.e., SCH66336 (Sarasar), BMS-214662, and R115777 (Zarnestra), which have reached clinical testing (21, 22), RPR-115135, a new non-peptidomimetic compound (26, 32, 33), and Manumycin (a natural compound)] were studied in human MPM cell lines, in short-term normal mesothelial cells, and in MPM cells in primary culture. In MTS assay, MPM cell lines were very resistant to the effect of all FTIs (Table 2). Only BMS-214662 was moderately active; hence, it was less active than in the human colon cancer cell line HCT116 or in the NSCLC cell line A549 (from 20- to 60-fold).

In short-term human normal mesothelial cells the IC_{25} was not reached after administration of each drug under test (Table 3).

Effects on human MPM cells in primary culture were evaluated on soft agar. Cells obtained from human samples were more resistant than cell lines. Although BMS-214662 was the only active drug among the five tested, its activity was drastically reduced (from 195- to 480-fold in comparison with HCT116 cells; Table 4).

Methotrexate, one of the oldest chemotherapeutic drugs, may work, in part, by inhibiting carboxyl methylation of Ras (34, 35). Methotrexate was studied in human MPM cell lines and in MPM cells in primary culture. Both MPM cell lines (Table 2, MTS assay) and MPM cells in primary culture (Table 4, soft agar assay) were very sensitive to the effect of this drug.

To gain insight into the mechanisms of cell inhibition induced by BMS-214662, its possible effect on apoptosis induction was studied. MPM cells were treated with the respective IC_{50} for 10 days. The ApopTag peroxidase *in situ* apoptosis assay revealed that BMS-214662 triggers moderate apoptosis in MPM cells (Fig. 3); only a fraction corresponding to 30% of all MPM cells presented the typical features of apoptosis. Gel ladder confirmed these data (Fig. 4).

Effects of FTIs on EGFR Ligand Release. The release of TGF-α was measured after treatment with two different FTIs, namely, BMS-214662 (moderately active) and RPR-115135 (nonactive). Both drugs did not affect the release of TGF-α in
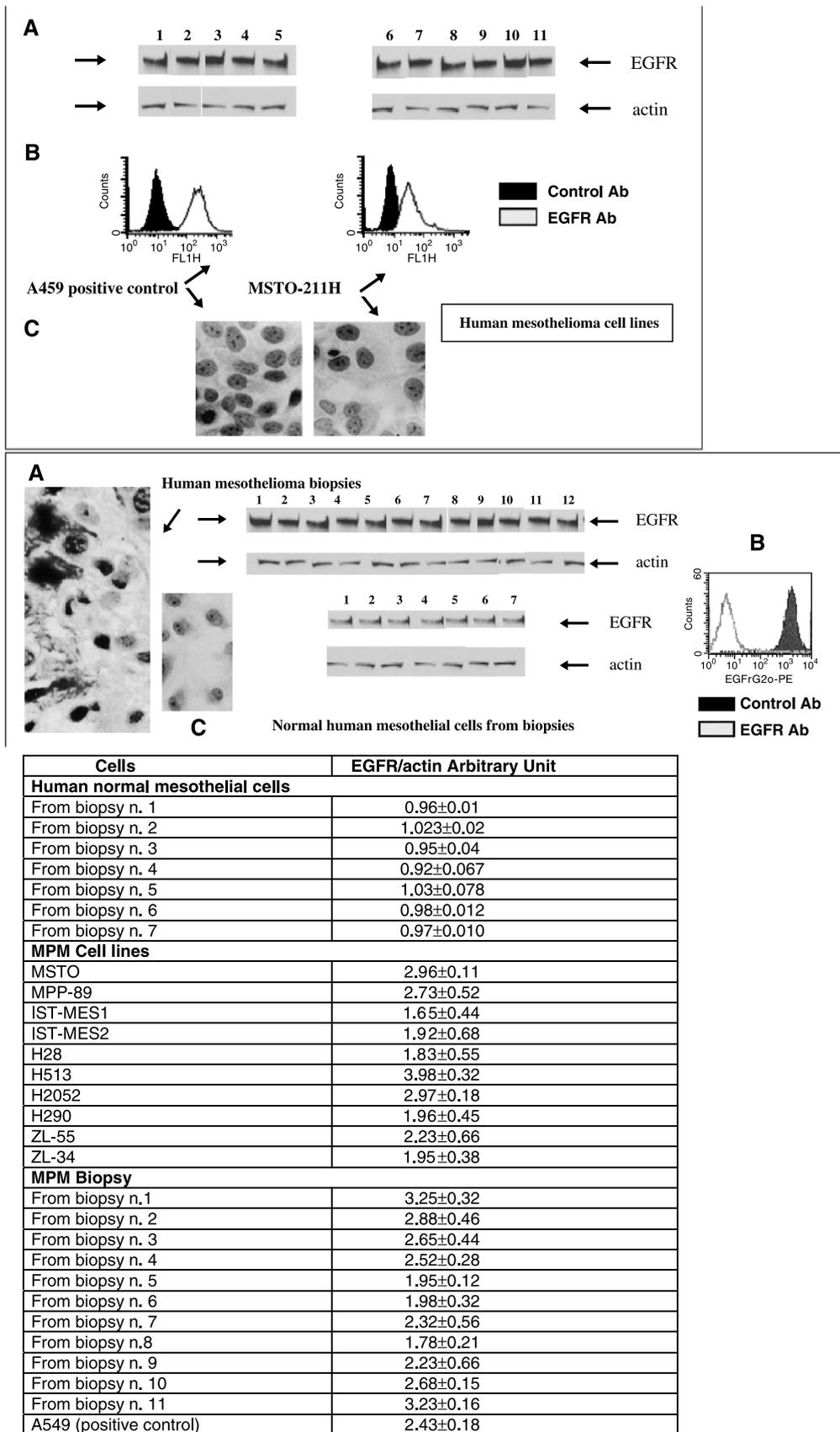
Fig. 2 Expression of EGFR in human mesothelioma cell lines, in human mesothelioma biopsies, and normal human biopsies of mesothelial cells. Top: *A,* Western blotting for EGFR and actin: 1, MSTO cell line; 2, MPP89; 3, IST-MES1; 4, IST-MES2; 5, H28; 6, H513; 7, H2052; 8, H290; 9, Zl-55; 10, ZL-34, 11. A549 (positive control). *B,* EGFR evaluates with cell flow (two cell lines as an example). *C,* immunohistochemistry (two cell lines as an example). Middle: *A,* Western blotting for EGFR and actin in human mesothelial biopsies: 1, A549 (positive control); 2 to 12, from different samples. *A,* Western blotting for EGFR and actin in normal human mesothelial biopsies: from 1 to 7 different samples. *B,* EGFR evaluates with cell flow (as an example). *C,* immunohistochemistry (as an example). Bottom: quantitative analysis of the intensity of the bands was done and the table shows the EGFR/actin ratio (in arbitrary units).

Cells	EGFR/actin Arbitrary Unit
Human normal mesothelial cells	
From biopsy n. 1	0.96±0.01
From biopsy n. 2	1.023±0.02
From biopsy n. 3	0.95±0.04
From biopsy n. 4	0.92±0.067
From biopsy n. 5	1.03±0.078
From biopsy n. 6	0.98±0.012
From biopsy n. 7	0.97±0.010
MPM Cell lines	
MSTO	2.96±0.11
MPP-89	2.73±0.52
IST-MES1	1.65±0.44
IST-MES2	1.92±0.68
H28	1.83±0.55
H513	3.98±0.32
H2052	2.97±0.18
H290	1.96±0.45
ZL-55	2.23±0.66
ZL-34	1.95±0.38
MPM Biopsy	
From biopsy n.1	3.25±0.32
From biopsy n. 2	2.88±0.46
From biopsy n. 3	2.65±0.44
From biopsy n. 4	2.52±0.28
From biopsy n. 5	1.95±0.12
From biopsy n. 6	1.98±0.32
From biopsy n. 7	2.32±0.56
From biopsy n.8	1.78±0.21
From biopsy n. 9	2.23±0.66
From biopsy n. 10	2.68±0.15
From biopsy n. 11	3.23±0.16
A549 (positive control)	2.43±0.18

Table 1 Release of TGF-α, amphiregulin, and EGF from primary pleural mesothelial cells, MPM, cell lines and primary culture

Cells	TGF-α (pg/mL)	Amphiregulin (pg/mL)	EGF (pg/mL)
HNMC			
From biopsy n.1	10	21.1 ± 0.4	33.1 ± 1.4
From biopsy n. 2	11 ± 0.4	21.4 ± 0.3	34.4 ± 2.3
From biopsy n. 3	18 ± 2.5	21.6 ± 0.2	32.8 ± 0.6
From biopsy n. 4	10	21.6 ± 0.4	31.9 ± 0.5
From biopsy n. 5	16 ± 1.2	21.9 ± 0.8	33.9 ± 2.6
From biopsy n. 6	18 ± 2.2	22.8 ± 1.5	33.8 ± 0.5
From biopsy n. 7	10	22.6 ± 1.7	34.6 ± 1.2
MPM cell lines			
MSTO	280 ± 15.6	244 ± 22.4	332 ± 42.6
MPP-89	122 ± 14.1	102 ± 12.6	142 ± 11.4
IST-MES1	180 ± 16.2	108 ± 26.4	188 ± 16.1
IST-MES2	110 ± 18.2	98 ± 8.4	178 ± 4.5
H28	150 ± 25.7	115 ± 29.3	178 ± 22.3
H513	130 ± 11.1	101 ± 17.8	161 ± 22.3
H2052	140 ± 35.6	87 ± 22.4	107 ± 39.6
H290	190 ± 5.9	104 ± 15.9	144 ± 35.9
ZL-55	170 ± 21.7	104 ± 31.5	124 ± 21.8
ZL-34	110 ± 44.8	80 ± 24.4	95 ± 14.8
MPM biopsy			
From biopsy n.1	211 ± 25.8	262 ± 14.2	322 ± 24.7
From biopsy n. 2	132 ± 13.1	102 ± 10.0	132 ± 17.2
From biopsy n. 3	142 ± 18.9	108 ± 26.5	138 ± 16.2
From biopsy n. 4	140 ± 14.1	114 ± 15.5	144 ± 25.7
From biopsy n. 5	280 ± 22.4	215 ± 35.2	284 ± 25.7
From biopsy n. 6	264 ± 11.6	166 ± 31.4	185 ± 42.4
From biopsy n. 7	245 ± 25.1	214 ± 36.1	245 ± 46.8
From biopsy n. 8	184 ± 12.6	155 ± 18.2	221 ± 15.8
From biopsy n. 9	241 ± 10.8	144 ± 1.8	165 ± 12.2
From biopsy n. 10	175 ± 21.4	178 ± 24.4	228 ± 26.1
From biopsy n. 11	211 ± 5.8	152 ± 11.1	202 ± 16.5
Positive control			
A549	248 ± 24.6	211 ± 44.8	311 ± 14.4

NOTE. Cells were cultured for 96 hours. Then the cell medium was assayed by ELISA for EGF and EGF-ligands. Data are the mean of duplicate determinations.

normal pleural mesothelial cells. In MPM cells, BMS-214662 moderately reduced (from 11% to 33%) the release of TGF-α in the culture medium. RPR-115135, on the contrary, increased the level of its release (Table 5). In the NSCLC A549 positive control, both drugs drastically reduced the release of TGF-α in the culture medium.

Effects of FTIs on HDJ2 Prenylation. When MPM cells were exposed to BMS-214662, SCH66336, R11577, RPR-115135 or Manumycin for 24 hours at the concentrations reported in Table 2 or in Table 4, a mobility shift on SDS-PAGE was observed in HDJ2 (Fig. 5), reflecting inhibition of FTase. In agreement with results previously reported by Kurzrock et al. (36), our data show that growth inhibition did not occur despite the substantial inhibition of FTase enzymatic activity.

Ras Activation. To determine whether EGF could enhance activity of Ras, a Ras activation assay was done using cell lysates of serum-starved cells.

The effect of EGF on Ras loading of GTP was examined in normal human mesothelial cells and compared with MPM cells. As shown in Fig. 6, in normal human mesothelial cells, EGF-induced Ras loading was detectable almost equally at both low (1 ng/mL) and high concentrations of EGF (100 ng/mL). Whereas Ras loading was efficient at low concentrations of EGF in MPM cells, surprisingly, stimulation with a high concentration (100 ng/mL) of EGF failed to activate Ras in these cells.

The activation of the ERKs is an important step in growth factor–induced mitogenic signal transduction. We find that EGF-induced ERK activation is significantly attenuated in MPM cells that overexpress the EGFR. ERK activation was determined by using an anti–phospho-ERK antibody in Western blots. This antibody recognizes phosphorylated forms of both ERK1 and ERK2. In normal mesothelium cells, EGF-induced ERK activation was high at low concentrations of EGF (1 ng/mL) and increased slightly at a high EGF concentration (100 ng/mL). In MPM cells, ERK activation was attenuated at all concentrations tested (Fig. 7) and did not increase at high concentration.

DISCUSSION

Consistently with previous reports (9–11), we showed that EGFR was overexpressed in MPM cells compared with normal pleural mesothelial cells. We showed that EGFR protein was expressed in MPM cells at a level equivalent to that of the A549 cell line derived from a patient with NSCLC. Numerous groups reported that EGFR was expressed and activated in A549 (37, 38). MPM cells constitutively expressed several EGFR ligands such as EGF, TGF-α, and amphiregulin. All of these

Table 2 Values of IC_{50} or IC_{25} (μmol/L) in human MPM cell lines evaluated after 10 days of uninterrupted treatment in MTS assay

Cell lines	BMS-214662	SCH66336	R115777	RPR-115135	Manumycin	Methotrexate
MSTO	1.48 ± 0.5	30 ± 0.0	21.8 ± 2.6	>30 [IC_{25}]	>30 ± 0.0 [IC_{25}]	0.007 ± 0.004
MPP-89	1.21 ± 0.01	30 ± 0.0	30 ± 0.0 [IC_{25}]	>30 [IC_{25}]	28.2 ± 1.8 [IC_{25}]	0.014 ± 0.008
IST-MES1	1.00 ± 0.5	30 ± 0.0 [IC_{25}]	27.2 ± 2.6 [IC_{25}]	>30 [IC_{25}]	29.2 ± 2.6 [IC_{25}]	0.015 ± 0.004
IST-MES2	1.68 ± 0.02	22.0 ± 4.6	3.4 ± 0.6 [IC_{25}]	>30 [IC_{25}]	28.7 ± 1.5 [IC_{25}]	0.009 ± 0.007
H28	1.18 ± 0.01	1.7 ± 0.3	3.1 ± 0.7	>30 [IC_{25}]	26.3 ± 2.6 [IC_{25}]	0.008 ± 0.003
H513	1.40 ± 0.05	15.5 ± 2.3	27.7 ± 2.9	>30 [IC_{25}]	29 ± 1.5 [IC_{25}]	0.005 ± 0.002
H2052	2.98 ± 0.8	14.5 ± 2.1 [IC_{25}]	>30 [IC_{25}]	>30 [IC_{25}]	>30 [IC_{25}]	0.015 ± 0.008
H290	3.5 ± 0.4	12.4 ± 3.1 [IC_{25}]	30 ± 0.0 [IC_{25}]	>30 [IC_{25}]	>30 [IC_{25}]	0.006 ± 0.004
ZL-55	1.8 ± 1.1	13.1 ± 2.4 [IC_{25}]	10 ± 1.3 [IC_{25}]	>30 [IC_{25}]	>30 [IC_{25}]	0.018 ± 0.01
ZL-34	1.2 ± 2.2	15.8 ± 1.6 [IC_{25}]	30 ± 0.0 [IC_{25}]	>30 [IC_{25}]	>30 [IC_{25}]	0.025 ± 0.06
HCT116*	0.06 ± 0.002	5.8 ± 3.8	1.30 ± 0.6	2.28 ± 0.8	0.52 ± 0.05	0.003 ± 0.001
A549*	0.04 ± 0.001	—	—	—	—	0.011 ± 0.003

NOTE. When the IC_{50} was not reached the IC_{25} was calculated (extrapolated as linear regression). Data are expressed as the mean ± SE of at least three independent experiments, each done in duplicate.

*Human colon cancer cell line HCT116 and human NSCLC cell line A549 were considered as a standard sensitive control for FTI action.

Table 3   Values of IC$_{25}$ (μmol/L) in human short-term culture of normal epithelium cells evaluated after 10 days of uninterrupted treatment in MTS assay

HNMC	BMS-214662	SCH66336	R115777	RPR-115135	Manumycin
From biopsy n. 1	>30	>30	>30	>30	>30
From biopsy n. 2	>30	>30	>30	>30	>30
From biopsy n. 3	>30	>30	>30	>30	>30
From biopsy n. 4	>30	>30	>30	>30	>30
From biopsy n. 5	>30	>30	>30	>30	>30
From biopsy n. 6	>30	>30	>30	>30	>30
From biopsy n. 7	>30	>30	>30	>30	>30

NOTE. Data are expressed as the mean ± SE of at least three independent experiments, each done in duplicate.

ligands are made as membrane-spanning prohormones that are processed and released through regulated proteolysis. The current paradigm is that membrane-anchored growth factors act as juxtacrine regulators of cell-cell signaling (39, 40). The observations that MPM cells overexpress amphiregulin, EGFR, EGF, and TGF-α suggest that excessive EGFR activation can contribute to mesothelioma aggressiveness.

Nørgaard et al. (24, 25) have shown data suggesting that the potential clinical use of FTIs could be expanded to include cancers harboring activated receptor tyrosine kinases as well as those containing activated Ras. Thus, working with MMTV-TGF-α mice, they showed that L-744,832 induced reversible regression of mammary tumors that was paralleled by a decrease in serum levels of TGF-α secreted by the tumor cells.

We tested the activity of five different FTIs [i.e., SCH66336 (Sarasar), BMS-214662, R115777 (Zarnestra), which have reached clinical testing (21, 22), RPR-115135, a new non-peptidomimetic compound (26, 32, 33), and Manumycin (a natural compound)] on MPM cells. Growth of MPM cells was substantially not affected by treatment with these FTIs. Among these five, BMS-214662 was the only one moderately active. BMS-214662 triggered apoptosis in a small fraction of cells (not higher than 30%) that was paralleled by a slight decrease in the levels of TGF-α secreted by treated MPM cells.

Interestingly, MPM cells are sensitive to methotrexate. The antifolate methotrexate is one of the most successful drugs in cancer chemotherapy. Although its efficacy is widely attributed to a decrease in nucleotide biosynthesis (41), methotrexate is known to increase homocysteine. A potential mechanism for the detrimental effects of homocysteine is cellular hypomethylation from an increase in *S*-adenosylhomocysteine, an inhibitor of methyltransferases including isoprenylcysteine carboxyl methyltransferase (Icmt). Among the substrates of Icmt is Ras, and carboxyl methylation of Ras is important for proper plasma membrane localization and function (42, 43). Recent results (34) showed that after methotrexate treatment, Ras is mislocalized to the cytosol, and its signaling functions are impaired, suggesting that methotrexate has an additional mechanism of action that leads to an inhibition in Ras signaling. Proteins that terminate with a carboxyl-terminal CAAX motif, such as the Ras and RhoB proteins, undergo three sequential posttranslational processing events:

1. The cysteine (i.e., the C of the CAAX sequence) is isoprenylated by FTase or geranylgeranyltransferase type I.
2. The last three amino acids of the protein (i.e., the -AAX) are cleaved off by Rce1, an integral membrane protein of the endoplasmic reticulum.
3. The newly exposed isoprenylcysteine is methylated by an endoplasmic reticulum membrane–bound methyltransferase, Icmt.

These modifications render the C terminus of CAAX proteins more hydrophobic, facilitating binding to membranes (21, 22, 42, 43). A search for factors involved in the intracellular trafficking of Ras has identified a specific and prenylation-dependent interaction between tubulin/microtubules and K-Ras. It was found that the polylysine region of K-Ras located immediately upstream of the prenylation site is required for binding of K-Ras to microtubules. Removal of the three carboxyl-terminal amino acids of farnesylated K-Ras with the specific endoprotease Rce1 abolished its binding to

Table 4   Values of IC$_{50}$ or IC$_{25}$ (μmol/L) in human mesothelioma cells in primary culture obtained by human biopsies evaluated after 10 days of uninterrupted treatment in soft agar

MPM biopsy	BMS-214662	SCH66336	R115777	RPR-115135	Manumycin	Methotrexate
n. 1	28.8 ± 1.4	4.5 ± 0.9 [IC$_{25}$]	12.5 ± 2.6 [IC$_{25}$]	>30	25.2 ± 1.1 [IC$_{25}$]	0.017 ± 0.02
n. 2	27.0 ± 1.3	12.1 ± 2.4 [IC$_{25}$]	11 ± 3.1 [IC$_{25}$]	>30	27.2 ± 0.3 [IC$_{25}$]	0.019 ± 0.07
n. 3	21.7 ± 0.4	5.0 ± 0.8 [IC$_{25}$]	>30 [IC$_{25}$]	>30	29 ± 1.3 [IC$_{25}$]	0.025 ± 0.04
n. 4	26.5 ± 1.1	4.0 ± 0.7 [IC$_{25}$]	4.2 ± 0.3 [IC$_{25}$]	>30	28 ± 1.2 [IC$_{25}$]	0.009 ± 0.002
n. 5	28.7 ± 0.7	30 ± 0.0 [IC$_{25}$]	30 ± 0.0 [IC$_{25}$]	>30	22.2 ± 0.5 [IC$_{25}$]	0.018 ± 0.03
n. 6	22.1 ± 4.2	30 ± 0.0 [IC$_{25}$]	30 ± 0.0 [IC$_{25}$]	>30	26.0 ± 0.7 [IC$_{25}$]	0.015 ± 0.03
n. 7	24.5 ± 1.6	14.0 ± 1.5 [IC$_{25}$]	14.6 ± 1.3 [IC$_{25}$]	>30	28 ± 1.2 [IC$_{25}$]	0.025 ± 0.07
n. 8	29.5 ± 1.4	22.2 ± 1.5 [IC$_{25}$]	25.3 ± 0.8 [IC$_{25}$]	>30	>30.0 [IC$_{25}$]	0.009 ± 0.002
n. 9	27.5 ± 0.4	30 ± 0.0 [IC$_{25}$]	30 ± 0.0 [IC$_{25}$]	>30	>30.0 [IC$_{25}$]	0.028 ± 0.01
n. 10	26.5 ± 1.8	300 ± 0 [IC$_{25}$]	30 ± 0.0 [IC$_{25}$]	>30	>30.0 [IC$_{25}$]	0.032 ± 0.08
n. 11	30 ± 0.0	30 ± 0.0 [IC$_{25}$]	30 ± 0.0 [IC$_{25}$]	>30	>30.0 [IC$_{25}$]	0.017 ± 0.02

NOTE. When the IC$_{50}$ was not reached the IC$_{25}$ was calculated (extrapolated as linear regression). Data are expressed as the mean ± SE of at least three independent experiments, each done in duplicate.

Cell lines	% apoptotic cells	MPM Biopsy	% apoptotic cells
MSTO	28.7±2.5	n.1	33.9±4.3
MPP-89	32.3±3.8	n.2	32.3±4.8
IST-MES1	35.7±1.7	n.3	29.9±1.6
IST-MES2	28.5±2.8	n.4	26.1±3.2
H28	32.7±4.4	n.5	31.6±2.8
H513	27.5±1.3	n.6	25.7±2.2
H2052	31.4±4.6	n.7	33.2±2.3
H290	33.6±3.4	n.8	32.3±5.4
ZL-55	31.1±1.9	n.9	31.2±1.8
ZL-34	26.2±3.5	n.10	26.1±2.2
HCT116 (positive control)	72.3±3.8	n.11	31.1±3.4
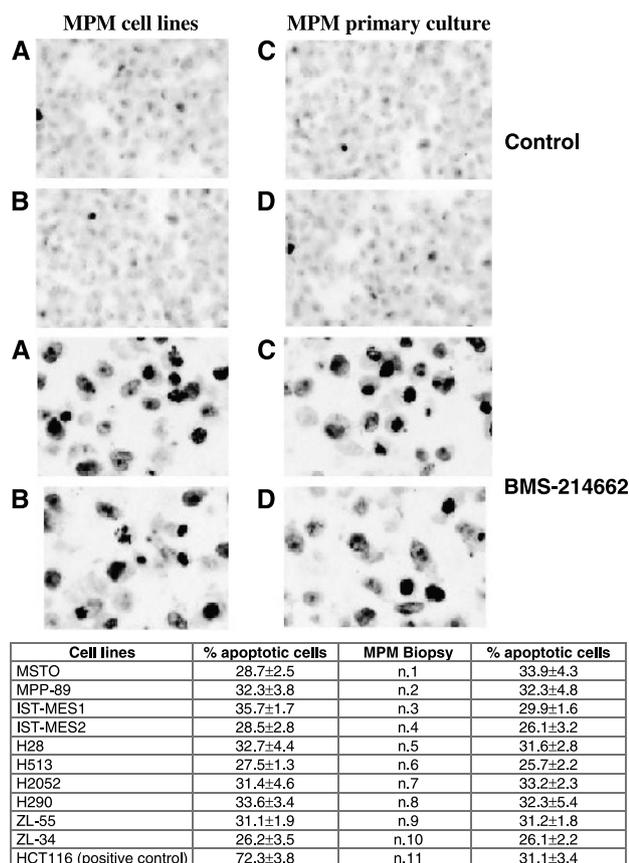
Fig. 3 Detection of apoptosis by ApopTag staining (representative figure from independent experiments) of MPM cell lines and of MPM in primary culture treated with the respective IC$_{50}$ of BMS-214662 for 10 days and stained after 24 hours' incubation in drug-free medium. The nuclei of apoptotic cells were stained dark brown. *A,* MSTO; *B,* MPP89; *C,* from biopsy n. 1; *D,* from biopsy n.2. The table reports the percentage (over controls) of apoptotic cells.

microtubules. Interestingly, however, methylation of the carboxyl-terminal prenylcysteine restored binding (43).

A potential drawback of the clinical use of FTIs is that K-Ras and N-Ras (the isoforms most often mutated in human tumors) can be efficiently geranylgeranylated in the setting of FTI therapy (21, 22). This alternate prenylation of the Ras proteins could limit the efficacy of FTIs in the treatment of Ras-induced tumors. The existence of an alternate means for prenylation has led several groups to focus on the postisoprenylation steps mediated by Rce1 and Icmt because those steps are shared by farnesylated and geranylgeranylated CAAX proteins (34, 35).

In our study all the five drugs inhibited the farnesylation of HDJ2 protein. Although the inhibition of HDJ2 farnesylation may indicate that these drugs are truly affecting their intended target, FTase, the degree of concordance between the farnesylation status of the HDJ2 chaperone protein, Ras, and/or other farnesylated proteins that are linked to clinical end points is not known. Therefore, serial evaluations of HDJ2 farnesylation may be used as general pharmacodynamic indices of protein farnesylation; however, concordant studies relating the farnesylation of HDJ2 to that of proteins linked to tumor proliferation are necessary to

determine the overall use and significance of such assessments. Indeed, Kurzrock et al. (36) reported that tumor inhibition did not occur despite the substantial inhibition of FTase enzymatic activity. Interestingly, the results of preclinical and clinical studies of the effects of L-778,123, an inhibitor of FTase, as well as geranylgeranyltransferase type I (to a lesser degree) on various prenylated proteins clearly showed that the agent was highly capable of inhibiting HDJ2 farnesylation, whereas the prenylation of K-Ras was not affected (44). Although these results are likely explained by the alternate prenylation of N- and K-Ras by residual geranylgeranyltransferase type I, they illustrate the lack of correlation between the inhibition of FTase activity and Ras functionality. A final issue pertaining to assessing the farnesylation status of HDJ2 and other proteins (i.e., Lamin B) that might
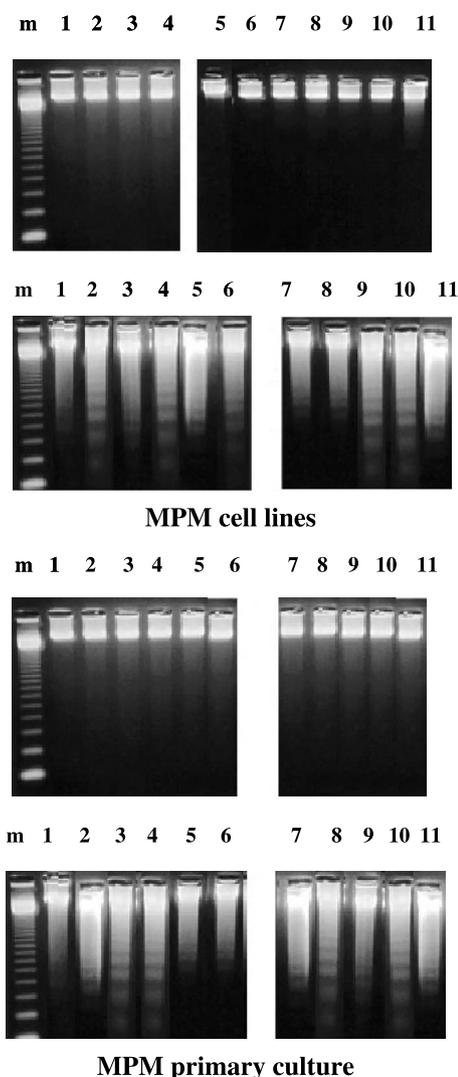
Fig. 4 Induction of apoptosis evaluated by internucleosomal DNA fragmentation (gel ladder). MPM cell lines and MPM in primary culture were treated with the respective IC$_{50}$ of BMS-214662 for 10 days. Representative of three replicate experiments yielding similar results. Top, untreated cells; bottom, treated cells. m, marker. MPM cell lines: 1, MSTO cell line; 2, MPP89; 3, IST-MES1; 4, IST-MES2; 5, H28; 6, H513; 7, H2052; 8, H290; 9, Zl-55; 10, ZL-34; 11, HCT116 (positive control). MPM primary culture from 1 to 11 different samples.

Table 5   Release of TGF-α from primary pleural mesothelial cells, MPM cell lines, and primary culture

Cells	BMS-214662	RPR-115135
HNMC		
From biopsy n. 1	14 ± 1.3	10
From biopsy n. 2	16 ± 1.4	10
From biopsy n. 3	14 ± 1.8	19 ± 2.7
From biopsy n. 4	10	11 ± 0.4
From biopsy n. 5	17 ± 19	13 ± 1.7
From biopsy n. 6	14 ± 1.3	21 ± 3.3
From biopsy n. 7	10	14 ± 0.6
MPM cell lines		
MSTO	211 ± 10.2* (−24.6)	395 ± 12.8* (41.1)
MPP-89	98 ± 4.1* (−19.7)	232 ± 13.5* (90.2)
IST-MES1	146 ± 1.2* (−18.9)	280 ± 26.7* (55.6)
IST-MES2	76 ± 8.7* (−31.0)	253 ± 38.1* (130)
H28	100 ± 15.4* (33.3)	232 ± 21.1* (54.7)
H513	98 ± 1.9* (−24.6)	260 ± 18.5* (100)
H2052	110 ± 15.1* (−21.4)	210 ± 41.6* (90.9)
H290	135 ± 15.7* (−29)	250 ± 15.8* (31.6)
ZL-55	135 ± 11.2* (−23.7)	242 ± 22.5* (79.3)
ZL-34	82 ± 16.8* (−25.4)	182 ± 24.6* (65.5)
MPM biopsy		
n.1	176 ± 25.8* (−16.6)	298 ± 35.1* (41.2)
n. 2	95 ± 18.6* (−28.0)	258 ± 23.4* (95.5)
n. 3	103 ± 8.2* (−27.5)	258 ± 17.2* (81.7)
n. 4	118 ± 17.6* (−15.7)	262 ± 19.2* (87.1)
n. 5	243 ± 12.3* (13.2)	397 ± 28.8* (41.8)
n. 6	242 ± 8.2* (−13.6)	395 ± 21.8* (41.1)
n. 7	217 ± 8.6* (−11.4)	428 ± 33.3* (74.7)
n.8	221 ± 16.4* (−19.3)	448 ± 16.7* (63.5)
n. 9	142 ± 17.3* (−16.5)	338 ± 18.8* (98.8)
n.10	138 ± 11.8* (−26.8)	411 ± 22.5* (42.6)
n. 11	198 ± 27.6* (6.6)	310 ± 33.5* (68.1)
Positive control		
A549*	55 ± 4.1* (−77.8)	85 ± 24.6* (65.7)

NOTE. Cells were cultured for 24 hours and then drug was added for following 48 hours. The cell medium was then assayed for TGF-α release by ELISA. Controls are reported in Table 1. Data are the mean of duplicate determinations. Values in parentheses are the percentage decrease or increase in the amount of TGF-α released in the medium after 48 hours' treatment.

*P = 0.05, statistically significant with respect to control values (reported in Table 1).

suffice as surrogates of relevant target effects is that the precise mechanism by which FTIs inhibit tumor proliferation and/or induce cytotoxicity is not known. This is shown by the responsiveness of cancers with both wild-type Ras and K-Ras mutations in preclinical studies and clear tumor regressions in patients with advanced malignancies with an inherently low incidence of Ras mutations including breast carcinoma, high-grade astrocytoma, and several types of hematopoietic malignancies (21, 22). In addition, one of the first studies on FTI action (45) showed that sensitivity/resistance was not related to the inability of the drug to inhibit the processing of Lamin B. Also, in our studies the ability of the drugs to inhibit the processing of HDJ2 protein is not correlated with MPM growth inhibition.

It is well known that the observed antitumor properties of FTIs are not solely due to Ras inhibition but may reflect inhibition of farnesylation. Prenylated proteins such as RhoB and centromere-associated CENP-E and -F have been proposed as the molecular targets of FTIs in all or some tumor cells (21, 22, 46). However, there remains no consensus as to the relevant target(s) of FTIs that can satisfactorily

account for the pharmacology of FTIs. BMS-214662, the only active drug among the five assayed, is the most potent apoptotic FTI known and exhibits curative responses in mice bearing a variety of staged human tumor xenografts such as HCT-116 human colon tumor (47, 48). A recent study (48) showed that BMS-214662 and BMS-225975, two tetrahydro-benzodiazepine-based FTIs that have nearly identical structures and very similar pharmacologic profiles associated with FTase inhibition, displayed different apoptotic property. BMS-225975 did not cause tumor regression and at best caused partial tumor-growth inhibition in staged HCT-116 human colon tumor xenografts. Lack of tumor regression activity in BMS-225975 was attributable to its relatively weak apoptotic potency, not to poor cell permeability or pharmacokinetics. The study concluded that it is very unlikely that FTase inhibition alone can account for the apoptotic potency of BMS-214662.
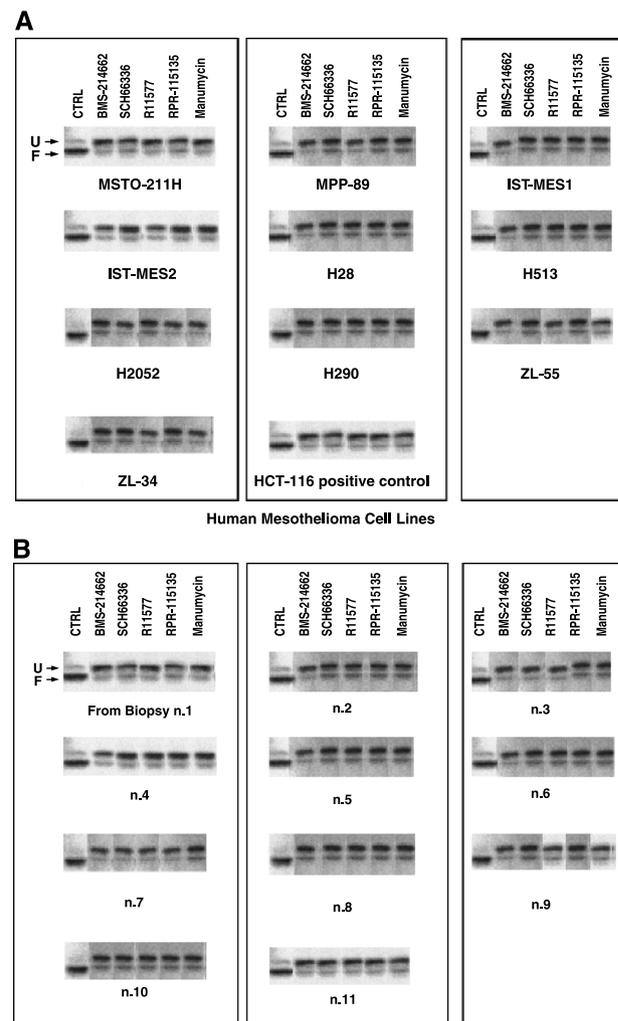
Fig. 5   Inhibition of farnesylation in MPM cells. *A,* cell lines; *B,* cells in primary culture obtained by biopsies. Extract from cells treated for 24 hours with FTIs were resolved by SDS-PAGE and protein detected by immunoblotting as described in Materials and Methods. CTRL, controls. Representative of three replicate experiments yielding similar results.

Fig. 6 Ras activation assays in response to EGF. Normal mesothelial cells were compared with MPM cells in primary cultures. The assay was done as described in Materials and Methods. Ras activation is impaired in MPM cells in primary cultures at high EGF concentrations (100 ng/mL). Cells were treated with EGF for 10 minutes. Representative of three replicate experiments yielding similar results.
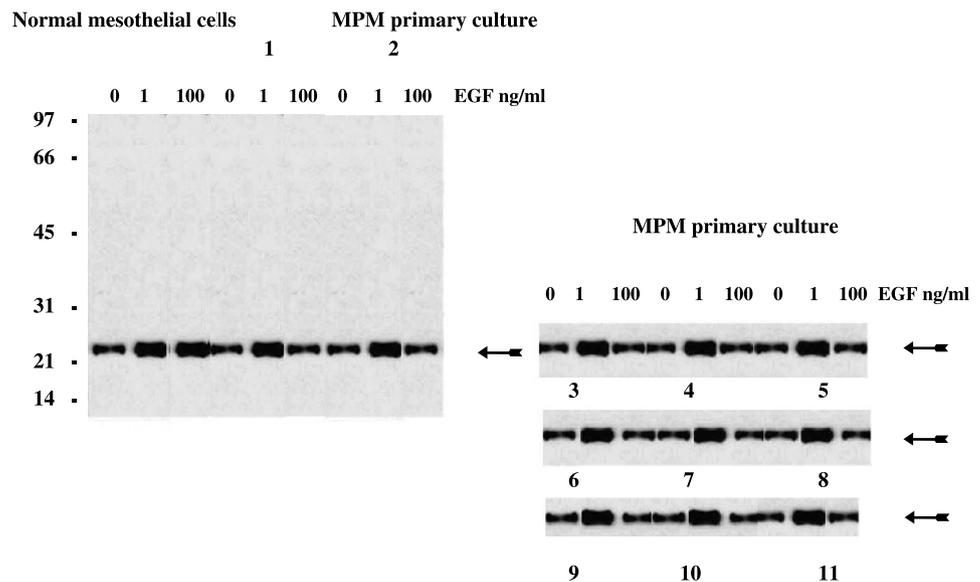
It is not clear at present if and how FTI-induced apoptosis is related to FTase inhibition in cells because no systematic attempt has been made to conduct studies at concentrations that are relevant to FTase inhibition and apoptosis. Manne et al. (48) reported that the BMS-214662 IC_{50} concentration able to inhibit the farnesylation of H-Ras or K-Ras was 1.3 and 8.4 nmol/L, respectively. This concentration is very close to that inducing apoptosis in human colon cancer cell line HCT-116 (0.1-1.0 μmol/L continuous exposure for 48 hours). In MPM cell lines and in MPM primary cells the IC_{50} values were in the range 1.0 to 4.0 μmol/L and 22.0 to 30.0 μmol/L, respectively. These concentrations induced apoptosis in ≈30% of cells after 10 days' continuous exposure. It may be possible to suppose that the BMS-214662–induced apoptosis in MPM would not be related to inhibition of farnesylation.

Exposure of cells to growth factors results in a rapid increase in GTP-bound Ras, which is the activated form of the protein. Activated Ras binds to a downstream kinase RAF, which in turn becomes activated (12–20). When we examined the effect of EGF concentration on Ras loading of GTP in normal pleural mesothelial cells and in MPM, we observed a different sensitivity. In normal cells, EGF-induced Ras loading was detectable almost equally at both low and high concentrations. Interestingly, in MPM cells, Ras activation was detectable at low concentrations of EGF whereas it was impaired at high EGF concentrations, suggesting that in these cells EGFR overexpression leads to alterations in EGF-induced Ras loading. ERK phosphorylation paralleled Ras activation by EGF; in normal mesothelium cells, EGF-induced ERK activation was high at low concentrations of EGF and increased slightly at a high EGF concentration. In MPM cells ERK activation was attenuated at all concentrations tested. It is, therefore, interesting to speculate that one mechanism of resistance involves the presence of Ras-independent mechanisms for growth factor activation of the mitogen-activated protein kinase signaling cascade. This mechanism might explain the resistance to FTI action.

As suggested by Habib et al. (40), an interesting general principle is that in cells expressing a high level of the EGFR, downstream signaling is strongly influenced by the concentration of EGF in the medium. Thus, increasing the expression of the EGFR might not result in a uniform alteration or

Fig. 7 Erk activation in response to EGF. Normal mesothelial cells were compared with MPM cells in primary cultures. The assay was done as described in Materials and Methods. Erk activation is impaired in MPM cells in primary cultures at high EGF concentrations (100 ng/mL). Cells were treated with EGF for 10 minutes. Representative of three replicate experiments yielding similar results.
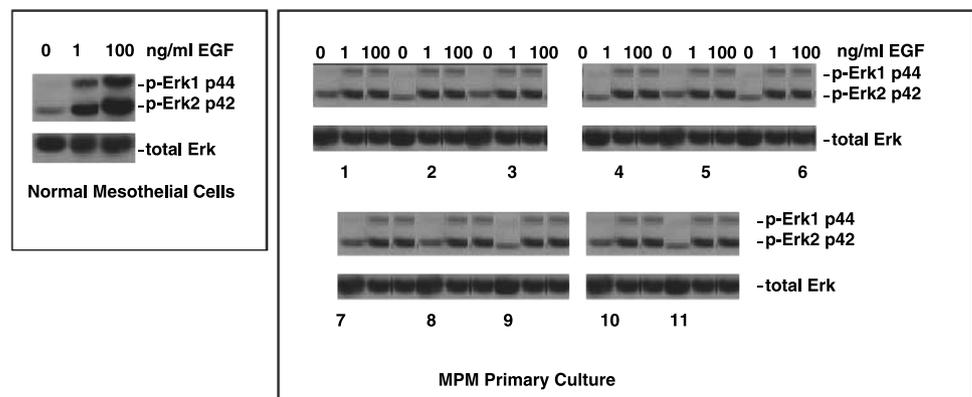
amplification of downstream signals. For example, even among signals that are attenuated, differences can be detected. In MPM cells, Ras activation is attenuated at high EGF concentrations.

Our data highlighted the concept that the same signaling pathway can be regulated in different ways and these regulations can differ between different cells of different origin. Furthermore, distinct signaling pathways cross talk with each other. Therefore, a compensatory pathway can emerge or selectively strengthen after inhibitors block one specific pathway. Different signaling pathways can control or affect the same cellular function, and one single signaling pathway can regulate different cellular functions. This apparently redundant cell signaling network actually may reflect a minor change mechanism for cells to respond and adjust to combined effects of simultaneous or sequential stimulation by many extracellular or internal signals and to control duration and intensity of each signal.

The results reported and commented in this article confirm the peculiar nature of MPM and add new information on its typical resistance to virtually any adopted chemotherapeutic strategy. The message we would like to draw from our experience is that by realizing a translational study, we have gathered from a single set of experiments a double set of information: an explanation for the clinical failure of drugs, together with a deeper basic knowledge on the disease.

Ideally, translational research is defined as the process of translating findings derived in basic science to the development of new understanding of disease mechanisms, diagnosis, and therapeutics. It is a functional bidirectional bridge among basic and clinical researchers realized through *ad hoc* collaborative efforts (48–53).

The data derived from our experience could help in planning future translational studies in MPM.

REFERENCES

1. Pelucchi C, Malvezzi M, La Vecchia C, Levi F, Decarli A, Negri E. The mesothelioma epidemic in Western Europe: an update. Br J Cancer 2004;90:1022–4.

2. Hemminki K, Li X. Mesothelioma incidence seems to have leveled off in Sweden. Int J Cancer 2003;103:145–6.

3. Peto J, Decarli A, La Vecchia C, Levi F, Negri E. The European mesothelioma epidemic. Br J Cancer 1999;79:666–72.

4. Cugell DW, Kamp DW. Asbestos and the pleura: a review. Chest 2004;125:1103–17.

5. van Ruth S, Baas P, Zoetmulder FA. Surgical treatment of malignant pleural mesothelioma: a review. Chest 2003;123:551–61.

6. Treasure T, Waller D, Swift S, Peto J. Radical surgery for mesothelioma. Br Med J 2004;328:237–8.

7. Sugarbaker DJ, Heher EC, Lee TH, et al. Extrapleural pneumonectomy, chemotherapy, and radiotherapy in the treatment of diffuse malignant pleural mesothelioma. J Thorac Cardiovasc Surg 1991; 102:10–4; discussion 14–5.

8. Vogelzang NJ, Rusthoven JJ, Symanowski J, et al. Phase III study of pemetrexed in combination with cisplatin versus cisplatin alone in patients with malignant pleural mesothelioma. J Clin Oncol 2003; 21:2636–44.

9. Trupiano JK, Geisinger KR, Willingham MC, et al. Diffuse malignant mesothelioma of the peritoneum and pleura, analysis of markers. Mod Pathol 2004;17:476–81.

10. Cai YC, Roggli V, Mark E, Cagle PT, Fraire AE. Transforming growth factor α and epidermal growth factor receptor in reactive and malignant mesothelial proliferations. Arch Pathol Lab Med 2004; 128:68–70.

11. Janne PA, Taffaro ML, Salgia R, Johnson BE. Inhibition of epidermal growth factor receptor signaling in malignant pleural mesothelioma. Cancer Res 2002;62:5242–7.

12. Yamada S, Taketomi T, Yoshimura A. Model analysis of difference between EGF pathway and FGF pathway. Biochem Biophys Res Commun 2004;314:1113–20.

13. Zhang T, Ma J, Cao X. Grb2 regulates Stat3 activation negatively in epidermal growth factor signalling. Biochem J 2003;376:457–64.

14. Cai T, Nishida K, Hirano T, Khavari PA. Gab1 and SHP-2 promote Ras/MAPK regulation of epidermal growth and differentiation. J Cell Biol 2002;159:103–12.

15. Saito T, Okada S, Ohshima K, et al. Differential activation of epidermal growth factor receptor (ErbB1/EGFR) downstream signaling pathways by betacellulin and EGF. Endocrinology 2004;149: 4232-43.

16. Holgado-Madruga M, Wong AJ. Role of the Grb2-associated binder 1/SHP-2 interaction in cell growth and transformation. Cancer Res 2004;64:2007–15.

17. Johnson GL, Lapadat R. Mitogen-activated protein kinase pathways mediated by ERK, JNK, and p38 protein kinases. Science 2002; 298:1911–2.

18. Cox AD, Der CJ. The dark side of Ras: regulation of apoptosis. Oncogene 2003;22:8999–9006.

19. Kinbara K, Goldfinger LE, Hansen M, Chou FL, Ginsberg MH. Ras GTPases: integrins' friends or foes? Nat Rev Mol Cell Biol 2003;4:767–76.

20. Herrmann C. Ras-effector interactions: after one decade. Curr Opin Struct Biol 2003;13:122–9.

21. Sebti SM, Adjei AA. Farnesyltransferase inhibitors. Semin Oncol 2004;31:28–39.

22. Russo P, Loprevite M, Cesario A, Ardizzoni A. Farnesylated proteins as anticancer drug targets: from laboratory to the clinic. Curr Med Chem Anti-Canc Agents 2004;4:123–38.

23. Sizemore N, Cox AD, Barnard JA, et al. Pharmacological inhibition of Ras-transformed epithelial cell growth is linked to down-regulation of epidermal growth factor-related peptides. Gastroenterology 1999; 117:567–76.

24. Norgaard P, Law BK, Plovisson HS, Moses HL. Farnesyltransferase inhibitor-induced regression of mammary tumors in TGF α and TGF α/neu transgenic mice correlates with inhibition of map kinase and p70s6 kinase phosphorylation. Ann N Y Acad Sci 1999;886: 265–8.

25. Norgaard P, Law B, Joseph H, et al. Treatment with farnesyl-protein transferase inhibitor induces regression of mammary tumors in transforming growth factor (TGF) α and TGF α/neu transgenic mice by inhibition of mitogenic activity and induction of apoptosis. Clin Cancer Res 1999;5:35–42.

26. Ottoboni C, Crippa A, Falugi C, Russo P. Induction of micronuclei by a new non-peptidic mimetic farnesyltransferase inhibitor RPR-115135: role of gene mutations. Mutagenesis 2001;16:423–30.

27. Trombino S, Cesario A, Margaritora S, et al. α7-Nicotinic acetylcholine receptors affect growth regulation of human mesothelioma cells: role of mitogen-activated protein kinase pathway. Cancer Res 2004;64:135–45. Erratum in Cancer Res 2004;64:1559.

28. Pass HI, Liu Z, Wali A, et al. Gene expression profiles predict survival and progression of pleural mesothelioma. Clin Cancer Res 2004; 10:849–59.

29. Gordon GJ, Jensen RV, Hsiao LL, et al. Using gene expression ratios to predict outcome among patients with mesothelioma. J Natl Cancer Inst 2003;95:598–605.

30. Gordon GJ, Jensen RV, Hsiao LL, et al. Translation of microarray data into clinically relevant cancer diagnostic tests using gene expression ratios in lung cancer and mesothelioma. Cancer Res 2002;62:4963–7.

31. Valente P, Arzani D, Cesario A, Margaritora S, Carbone E, Russo P. TNF increases camptothecin-induced apoptosis by inhibition of NF-κB. Eur J Cancer 2003;39:1468–77.

32. Russo P, Arzani D, Trombino S, Falugi C. c-myc down-regulation induces apoptosis in human cancer cell lines exposed to RPR-115135 (C31H29NO4), a non-peptidomimetic farnesyltransferase inhibitor. J Pharmacol Exp Ther 2003;304:37–47.

33. Russo P, Malacarne D, Falugi C, Trombino S, O'Connor PM. RPR-115135, a farnesyltransferase inhibitor, increases 5-FU-cytotoxicity in ten human colon cancer cell lines: role of p53. Int J Cancer 2002; 100:266–75.

34. Winter-Vann AM, Kamen BA, Bergo MO, et al. Targeting Ras signaling through inhibition of carboxyl methylation: an unexpected property of methotrexate. Proc Natl Acad Sci U S A 2003;100:6529–34.

35. Philips MR. Methotrexate and Ras methylation: a new trick for an old drug? Sci STKE 2004:225:pe13.

36. Kurzrock R, Kantarjian HM, Cortes JE, et al. Farnesyltransferase inhibitor R115777 in myelodysplastic syndrome: clinical and biologic activities in the phase 1 setting. Blood 2003;102:4527–34.

37. Ono M, Hirata A, Kometani T, et al. Sensitivity to gefitinib (Iressa, ZD1839) in non-small cell lung cancer cell lines correlates with dependence on the epidermal growth factor (EGF) receptor/extracellular signal-regulated kinase 1/2 and EGF receptor/Akt pathway for proliferation. Mol Cancer Ther 2004;3:465–72.

38. Janmaat ML, Kruyt FA, Rodriguez JA, Giaccone G. Response to epidermal growth factor receptor inhibitors in non-small cell lung cancer cells: limited antiproliferative effects and absence of apoptosis associated with persistent activity of extracellular signal-regulated kinase or Akt kinase pathways. Clin Cancer Res 2003;9:2316–26.

39. Burke P, Schooler K, Wiley HS. Regulation of EGF receptor signaling by endocytosis and intracellular trafficking. Mol Biol Cell 2001;12:1897–910.

40. Habib AA, Chun SJ, Neel BG, Vartanian T. Increased expression of epidermal growth factor receptor induces sequestration of extracellular signal-related kinases and selective attenuation of specific epidermal growth factor-mediated signal transduction pathways. Mol Cancer Res 2003;1:219–33.

41. Zhao R, Goldman ID. Resistance to antifolates. Oncogene 2003; 22:7431–57.

42. Young SG, Ambroziak P, Kim E, Clarke S. Postisoprenylation protein processing: C' (CaaX) endoproteases and isoprenylcysteine carboxyl methyltransferase. In: Tamanoi F, Sigman DS, editors. The enzymes. Vol. 21. San Diego (CA): Academic Press; 2000. p. 155–213.

43. Chen Z, Otto JC, Bergo MO, Young SG, Casey PJ. The C-terminal polylysine region and methylation of K-Ras are critical for the interaction between K-Ras and microtubules. J Biol Chem 2000; 275:41251–7.

44. Lobell RB, Liu D, Buser CA, et al. Preclinical and clinical pharmacodynamic assessment of L-778, 123, a dual inhibitor of farnesyl: protein transferase and geranylgeranyl:protein transferase type-1. Mol Cancer Ther 2002;1:747–58.

45. Sepp-Lorenzino L, Ma Z, Rands E, et al. A peptidomimetic inhibitor of farnesyl:protein transferase blocks the anchorage-dependent and -independent growth of human tumor cell lines. Cancer Res 1995; 55:5302–9.

46. Falugi C, Trombino S, Granone P, Margaritora S, Russo P. Increasing complexity of farnesyltransferase inhibitors activity: role in chromosome instability. Curr Cancer Drug Targets 2003;3:109–18.

47. Rose WC, Lee FY, Fairchild CR, et al. Preclinical antitumor activity of BMS-214662, a highly apoptotic and novel farnesyltransferase inhibitor. Cancer Res 2001;61:7507–17.

48. Manne V, Lee FY, Bol DK, et al. Apoptotic and cytostatic farnesyltransferase inhibitors have distinct pharmacology and efficacy profiles in tumor models. Cancer Res 2004;64:3974–80.

49. Cesario A, Galetta D, Russo P, Margaritora S, Granone P. The role of the surgeon in translational research. Lancet 2003;362:1082.

50. Yeatman TJ. The future of cancer management: translating the genome, transcriptome, and proteome. Ann Surg Oncol 2003;10: 7–14.

51. Kreeger K. From bench to bedside. Nature 2003;424:1090–1.

52. Apolone G. Clinical and outcome research in oncology. The need for integration. Health Qual Life Outcomes 2003;1:3.

53. Wong S, Witte ON. The BCR-ABL story: bench to bedside and back. Annu Rev Immunol 2004;22:247–306.